

Supporting Information

for

Modified-Graphene-Oxide-Containing Styrene Masterbatches for Thermosets

Siyao He,^a Yuqiang Qian,^c Kunwei Liu,^b Christopher W. Macosko,^{b,*} and Andreas Stein^{a,*}

a. Department of Chemistry, University of Minnesota, 207 Pleasant St. SE, Minneapolis, MN 55455, USA

b. Department of Chemical Engineering & Materials Science, University of Minnesota, 421 Washington Ave. SE, Minneapolis, MN 55455, USA

c. Adama Materials, 2000 University Ave. #602, East Palo Alto, CA 94303, USA

* Corresponding authors: a-stein@umn.edu, macosko@umn.edu

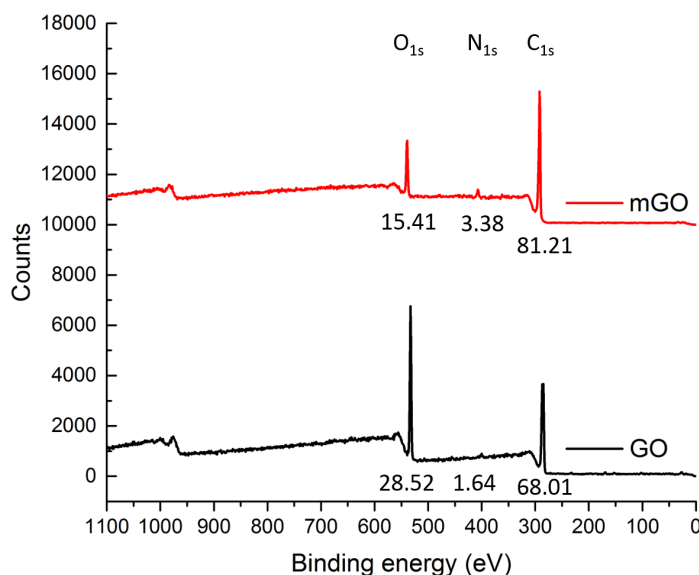


Figure S1. X-ray photoelectron spectroscopy data of pristine GO and modified GO. The number under each peak represents the abundance in atom percent of the corresponding element in the sample. The difference in nitrogen content between mGO and GO was used to estimate the fraction of dodecylamine in mGO. On the basis of the nitrogen content of mGO, the dodecylamine functional group accounts for about 27% of the total mass of mGO, which is lower than the value of 40% weight loss determined by TGA. The latter weight loss may include some loss of oxygen and carbon from GO during heating. Comparing the X-ray photoelectron spectroscopy results of GO and mGO, GO was reduced during modification. The C:O ratio changed from 2.38:1 to 5.27:1 (carbon from dodecylamine subtracted) after dodecylamine modification, which explains the reduction peak in the XRD pattern of mGO at $24^{\circ} 2\theta$ that is typically associated with chemically reduced GO.

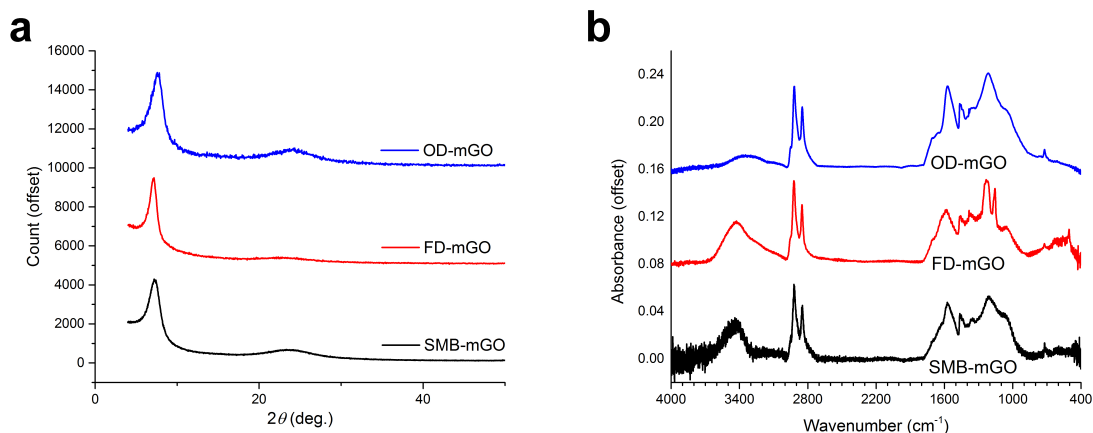


Figure S2. (a) XRD patterns and (b) IR spectra of differently processed mGO. The OD-mGO sample gives a slightly broader low-angle peak, which may indicate that the rapid drying process causes more disorder inside the aggregates. The additional IR absorption peak at 1159 cm^{-1} of the FD-mGO sample corresponds to the C–OH stretching vibration,¹ which originates from the hydroxyl groups on the GO surface that cannot be removed by room temperature freeze drying.

(1) Galande, C.; Mohite, A. D.; Naumov, A. V.; Gao, W.; Ci, L.; Ajayan, A.; Gao, H.; Srivastava, A.; Weisman, R. B.; Ajayan, P. M. Quasi-Molecular Fluorescence from Graphene Oxide. *Sci. Rep.* **2011**, *1*, 85.

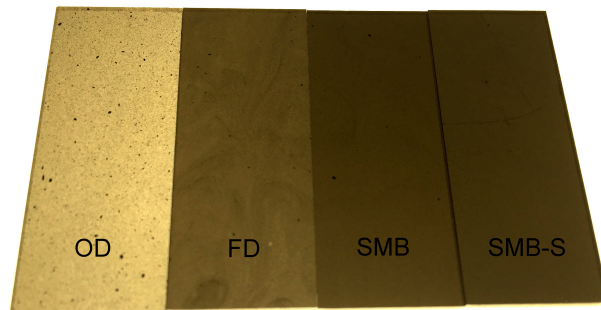


Figure S3. Photograph of 1.5 mm UP resin plaques containing 0.04 wt% mGO and prepared by the four different processes outlined in Figure 1 of the main manuscript. Note that the OD and FD samples contain visible particle aggregates, and they are lighter in color compared to SMB and SMB-S samples.

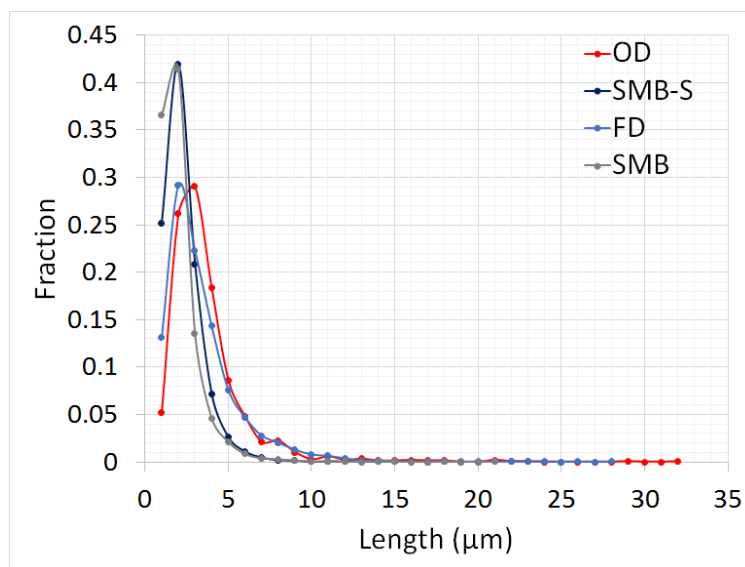


Figure S4. Particle size distributions of mGO aggregates in differently processed mGO/resin composites. Trendlines are used only to guide the reader's eyes. The total sampling area for each sample is 0.574 mm^2 . Total counts are 1564, 3425, 7734, and 7291 for the OD, FD, SMB, and SMB-S samples, respectively.

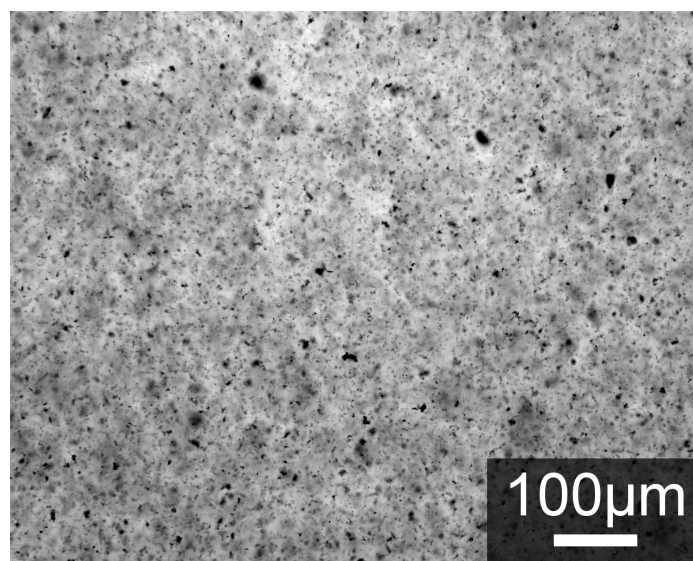


Figure S5. VLM micrograph of VE resin with 0.04 wt.% SMB mGO.

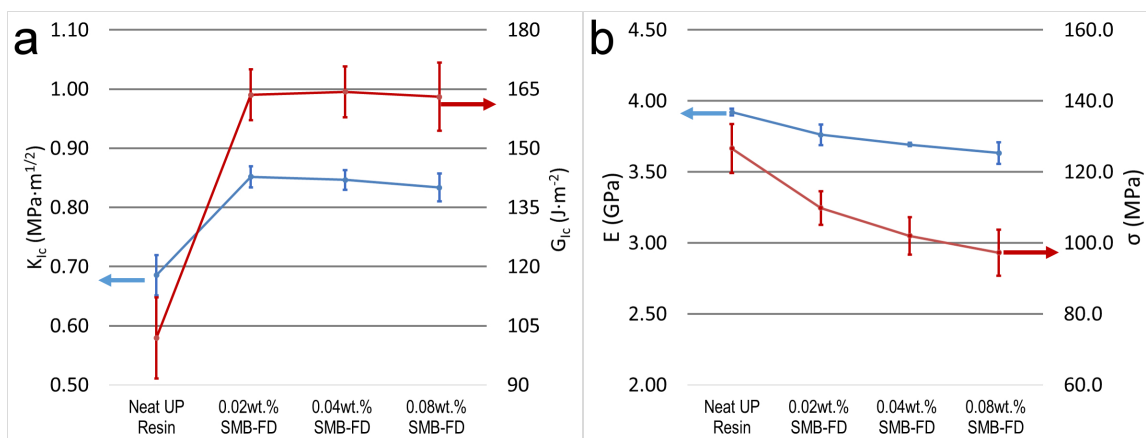


Figure S6. Mechanical properties of SMB-FD mGO/UP resin composites. (a) K_{IC} and G_{IC} , (b) flexural modulus and flexural strength.

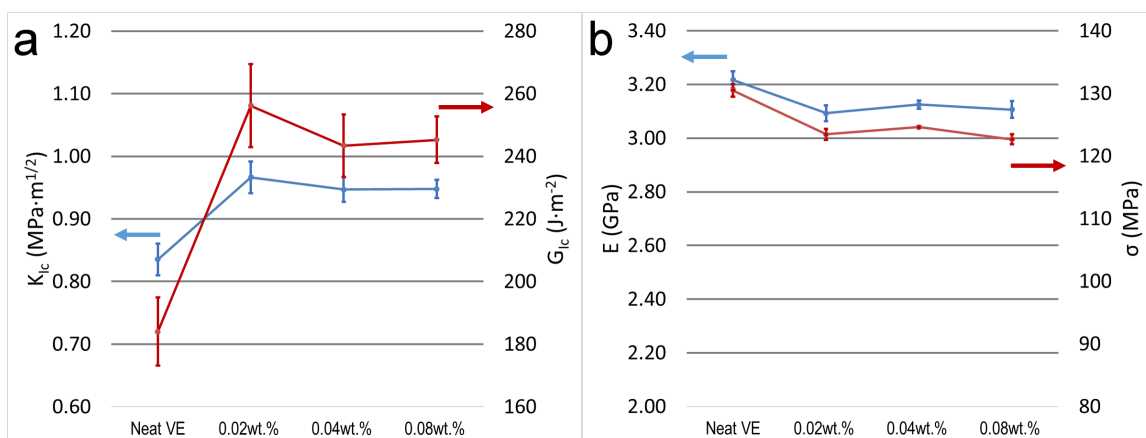


Figure S7. Mechanical properties of mGO/VE resin SMB composites. (a) K_{IC} and G_{IC} , (b) flexural modulus and flexural strength.

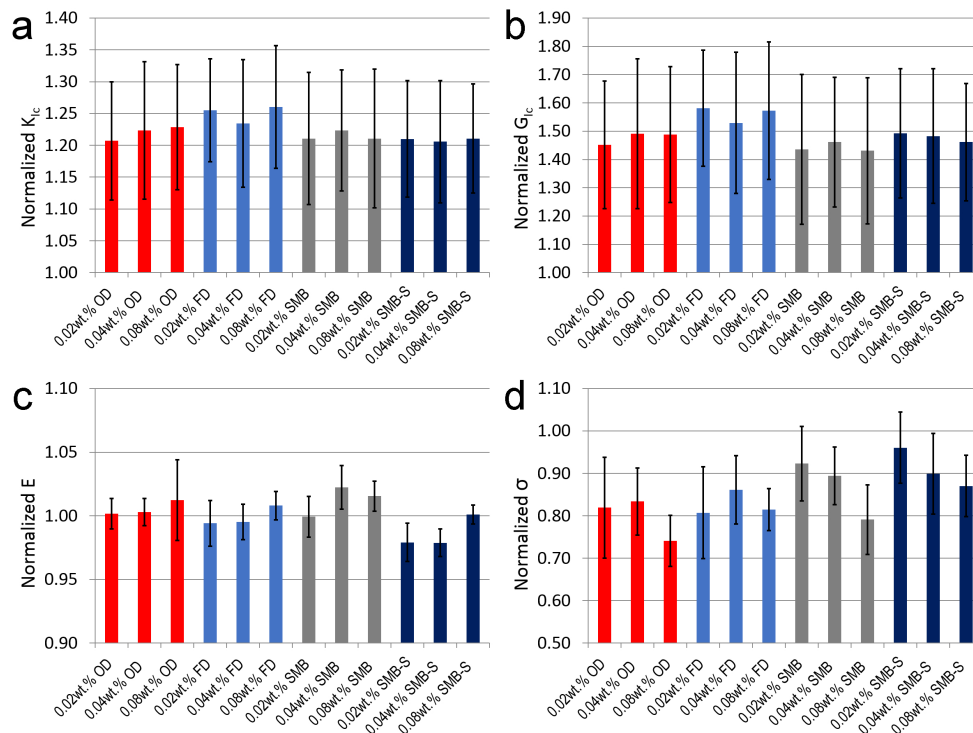


Figure S8. Mechanical properties of UP resin composites with differently processed mGO. (a) K_{IC} , (b) G_{IC} , (c) flexural modulus, and (d) flexural strength. All data are normalized to values of the neat UP resin.

Table S1. Mechanical properties of the UP resin composites normalized to the corresponding values of the neat UP resin.

| | K1c | StDev | G1c | StDev | Modulus | Stdev | Strength | Stdev |
|----------------|------|-------|------|-------|---------|-------|----------|-------|
| Neat UP Resin | 1.00 | 0.05 | 1.00 | 0.10 | 1.00 | 0.01 | 1.00 | 0.05 |
| 0.02wt.% OD | 1.21 | 0.09 | 1.45 | 0.23 | 1.00 | 0.01 | 0.82 | 0.12 |
| 0.04wt.% OD | 1.22 | 0.11 | 1.49 | 0.26 | 1.00 | 0.01 | 0.83 | 0.08 |
| 0.08wt.% OD | 1.23 | 0.10 | 1.49 | 0.24 | 1.01 | 0.03 | 0.74 | 0.06 |
| 0.02wt.% FD | 1.26 | 0.08 | 1.58 | 0.21 | 0.99 | 0.02 | 0.81 | 0.11 |
| 0.04wt.% FD | 1.23 | 0.10 | 1.53 | 0.25 | 1.00 | 0.01 | 0.86 | 0.08 |
| 0.08wt.% FD | 1.26 | 0.10 | 1.57 | 0.24 | 1.01 | 0.01 | 0.81 | 0.05 |
| 0.02wt.% SMB | 1.21 | 0.10 | 1.44 | 0.26 | 1.00 | 0.02 | 0.92 | 0.09 |
| 0.04wt.% SMB | 1.22 | 0.09 | 1.46 | 0.23 | 1.02 | 0.02 | 0.89 | 0.07 |
| 0.08wt.% SMB | 1.21 | 0.11 | 1.43 | 0.26 | 1.02 | 0.01 | 0.79 | 0.08 |
| 0.02wt.% SMB-S | 1.21 | 0.09 | 1.49 | 0.23 | 0.98 | 0.02 | 0.96 | 0.08 |
| 0.04wt.% SMB-S | 1.21 | 0.10 | 1.48 | 0.24 | 0.98 | 0.01 | 0.90 | 0.09 |
| 0.08wt.% SMB-S | 1.21 | 0.09 | 1.46 | 0.21 | 1.00 | 0.01 | 0.87 | 0.07 |

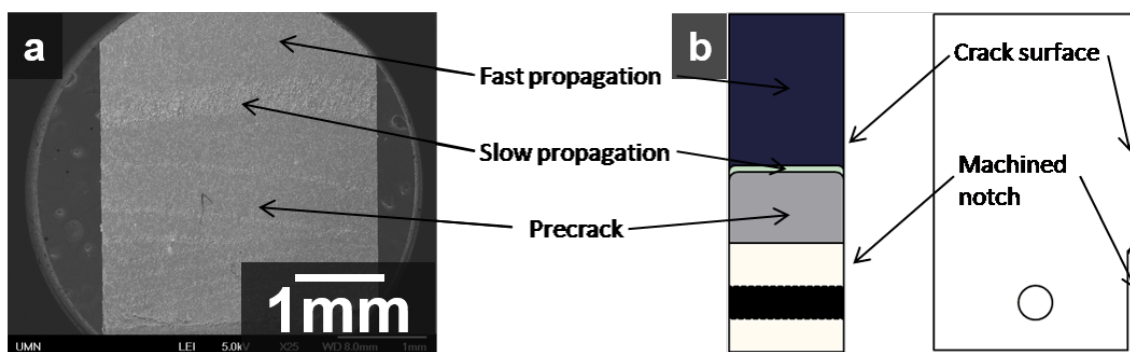


Figure S9. Definition of different regions on the crack surface. (a) Low magnification SEM image of a failed CT specimen. (b) A schematic of the crack surface.

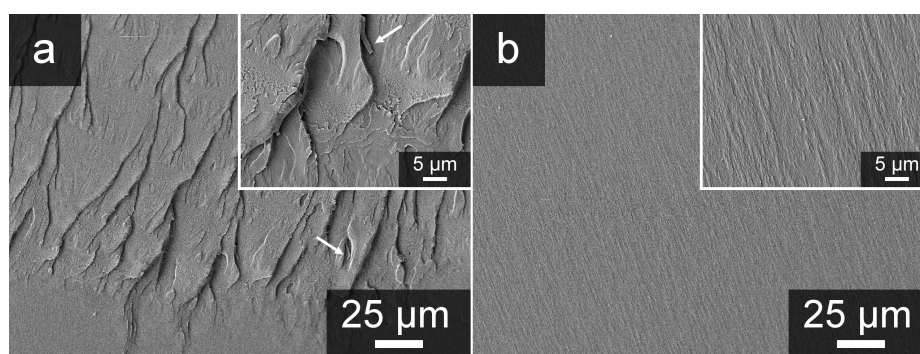


Figure S10. SEM fractographs of neat UP resin in the near precrack region (a) and fast propagation region (b). Crack propagation direction: from bottom to top.

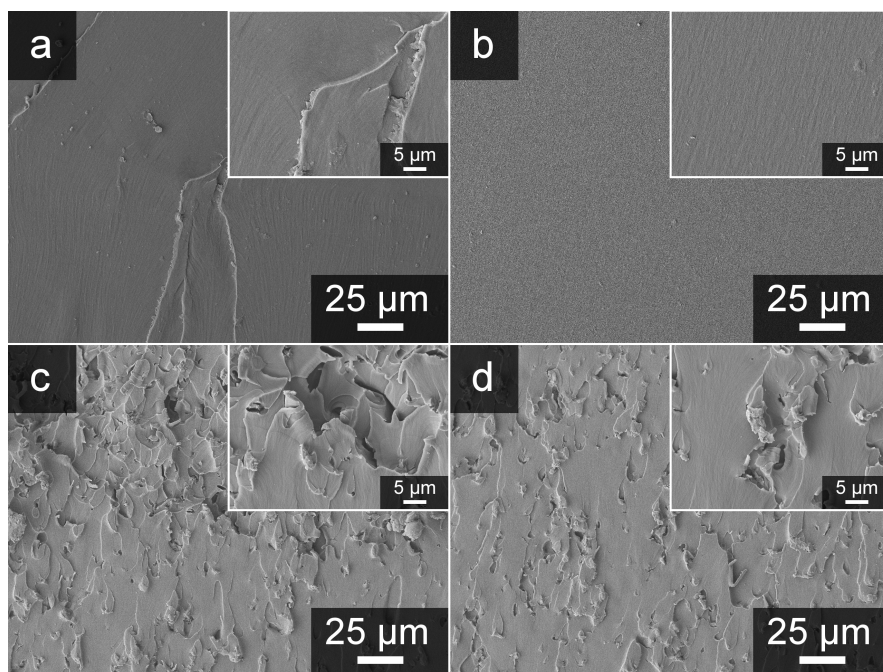


Figure S11. SEM fractographs of failed compact tension samples: neat VE resin (a, b), VE resin with 0.04 wt% mGO prepared by the SMB process (c, d). Positions in the specimens: near precrack (a, c), and fast propagation region (b, d). Crack propagation direction: from bottom to top.